Available online at www.sciencedirect.com
SCIENCE DIRECT
Journal of the European Ceramic Society 26 (2006) 2293–2299
www.elsevier.com/locate/jeurceramsoc

Polymorphism in the $Lu_{2-x}Y_xSi_2O_7$ system at high temperatures

A.I. Becerro *, A. Escudero

Departamento de Química Inorgánica, Instituto de Ciencia de Materiales de Sevilla, Universidad de Sevilla-CSIC, Avda. Américo Vespucio, s/n, 41092 Sevilla, Spain

Received 2 February 2005; received in revised form 23 March 2005; accepted 23 April 2005
Available online 5 July 2005

Abstract

Samples in the system $Lu_{2-x}Y_xSi_2O_7$ ($1.25 \leq \times \leq 2$) have been synthesised following a sol–gel method and calcined to high temperatures ($\geq$1400 °C). X-ray diffraction (XRD) has shown that all compositions crystallize as β-$Lu_{2-x}Y_xSi_2O_7$ at the low temperatures, while increasing calcination temperature produces the formation of the γ- and δ-polymorphs, the temperatures of formation of each polymorph depending on the Y/Lu ratio. Unit cell parameters of the samples crystallizing as γ-$Lu_{2-x}Y_xSi_2O_7$ have been calculated and plotted as a function of composition. They show a linear change with increasing Y content, indicating a degree of solid solubility of $Lu_2Si_2O_7$ in γ-$Y_2Si_2O_7$. Based on these data and on those reported in our previous studies [Becerro, A.I. and Escudero, A., XRD and ^{29}Si MAS NMR spectroscopy across the β-$Lu_2Si_2O_7$–β-$Y_2Si_2O_7$ solid solution. *J. Solid State Chem.*, 2005, **178**; Becerro, A.I. and Escudero, A., Phase transitions in Lu-doped $Y_2Si_2O_7$ at high temperatures. *Chem. Mater.*, 2005, **17**, 112] a temperature–composition diagram of the $Lu_2Si_2O_7$–$Y_2Si_2O_7$ system is given. Finally, the influence of Lu on the reversibility of the γ-$Y_2Si_2O_7$ → β-$Y_2Si_2O_7$ transition is studied by means of XRD and ^{29}Si MAS NMR spectroscopy.

Keywords: Sol–gel processes; X-ray methods; Structural applications; Silicate; Phase transitions; $(Lu,Y)_2Si_2O_7$

1. Introduction

Silicon nitride (Si_3N_4) has become an important class of materials for structural applications at high temperature.[1–5] However, it is difficult to sinter because of the low diffusivity of this covalent material.[6] Densification was initially achieved by liquid-phase sintering using MgO as the sintering additive;[7] however, it caused high temperature strength loss attributed to the formation of a vitreous silicate intergranular phase.[8,9] Much effort has been made to improve the high temperature mechanical properties of Si_3N_4 including the use of other oxides and subsequent crystallization of the intergranular glassy phase by a post-sintering heat treatment. It has been shown that when RE oxides (RE = lanthanides and yttrium) are added to the powder of pure Si_3N_4, a glassy disilicate phase ($RE_2Si_2O_7$) forms in the intergranular regions which, upon crystallization, improves the high-temperature mechanical properties of the material.[10–15] Knowledge of the crystalline structures adopted by the $RE_2Si_2O_7$ intergranular phase at different temperatures and RE contents is, therefore, of great value in understanding the behaviour of these materials. Several studies have shown that the high temperature strength and oxidation resistance of Si_3N_4 are correlated with the cationic radius of the RE cation in the oxide additives, such that the smaller the RE cation the better the properties of the Si_3N_4.[15,16] Y_2O_3, Lu_2O_3 and Sc_2O_3 are the three RE oxides showing the highest flexural strength values. We have selected the first two cations to examine the phase transitions with temperature and composition in the $Lu_2Si_2O_7$–$Y_2Si_2O_7$ system.

The academic interest of this study resides in the fact that $Lu_2Si_2O_7$ forms a unique polymorph in the whole temperature range, called β-$Lu_2Si_2O_7$, while $Y_2Si_2O_7$ shows up to five polymorphs with increasing temperature (*y*, α, β, γ and δ).[17,18] Transition temperatures between the different $Y_2Si_2O_7$ polymorphs as well as temperature stability ranges vary considerably from one author to the other.[12,19–24] Ito and Johnson[25] established the following sequence:

$$\alpha \overset{1225\,^\circ C}{\rightarrow} \beta \overset{1445\,^\circ C}{\rightarrow} \gamma \overset{1535\,^\circ C}{\longleftrightarrow} \delta$$

* Corresponding author. Tel.: +34 95 4489576; fax: +34 95 4460665.
E-mail address: anieto@icmse.csic.es (A.I. Becerro).

0955-2219/$ – see front matter © 2005 Elsevier Ltd. All rights reserved.
doi:10.1016/j.jeurceramsoc.2005.04.029

but direct transitions from y-$Y_2Si_2O_7$ to β-$Y_2Si_2O_7$ have also been reported.[14,26]

The study of phase transformations with temperature in the $Lu_{2-x}Y_xSi_2O_7$ member with $x = 1$ was recently reported by us;[27] the results show that at 1200 °C β-$RE_2Si_2O_7$ is formed, with Y and Lu sharing the RE crystallographic site and this polymorph is the stable phase up to, at least, 1650 °C. A second study on the $Lu_{2-x}Y_xSi_2O_7$ system describing the structures at 1300 °C shows that a complete solid solution exists between β-$Lu_2Si_2O_7$ and β-$Y_2Si_2O_7$ at that temperature.[28]

The present study analyses the phase transitions of $Lu_{2-x}Y_xSi_2O_7$ samples with high Y contents ($1.25 \leq \times \leq 2$) at high temperatures (1400 °C $\leq T \leq$ 1700 °C). Transition temperatures and evolution of lattice parameters with temperature and composition as well as reversibility of phase transitions have been studied with ex situ X-ray diffraction and ^{29}Si MAS NMR spectroscopy. Finally, a temperature–composition diagram of the $Lu_2Si_2O_7$–$Y_2Si_2O_7$ system is given, based on data presented in this article and in our previous studies.[27,28]

2. Experimental section

2.1. Synthesis of the xerogels

The sol–gel route used for this study was derived from the synthesis of a well-homogenized gel of $Y_2Si_2O_7$.[29] The starting materials were $Y(NO_3)_3{\cdot}6H_2O$ (99.9% Sigma), $Lu(NO_3)_3{\cdot}5H_2O$ (99.9% Sigma), $Si(OC_2H_5)_4$ (TEOS, 98% solution Sigma), HCl 35% aqueous solution and 96% ethanol. A TEOS solution in ethanol (1:3 in volume) was added over appropriate amounts of $Y(NO_3)_3{\cdot}6\ H_2O$, $Lu(NO_3)_3{\cdot}6\ H_2O$ and HCl for the preparation of $Lu_{2-x}Y_xSi_2O_7$ members with nominal $x = 1.25$, 1.50, 1.66, 1.80 and 2.00. The mixtures were stirred at 40 °C for 72 h and the transparent gels obtained were dried at 60 °C for 24 h in air. Nitrate was eliminated by calcination at 500 °C for 1 h at a heating rate of 1 °C/min.

2.2. Calcination experiments

The xerogel of each composition was divided into four portions and they were calcined at 1400, 1500, 1600 and 1650 °C for 12 h at a heating rate of 5 °C/min. Samples were slowly cooled down to room temperature. After characterization, each sample was subsequently calcined at the same temperature for another 24 h and slowly cooled down to room temperature.

2.3. Reversibility studies

To study the reversibility of the γ → β transition, the γ-polymorph of each composition was annealed for 240 h at 1300 °C, a temperature at which the β-polymorph is the stable phase for all five compositions.[27] Asterisks in Table 2 indicate samples submitted to the reversibility study.

Table 1
Nominal and real Y/(Y + Lu) and Si/(Y + Lu) ratios of the $Lu_{2-x}Y_xSi_2O_7$ samples

x	Y/(Y + Lu)		Si/(Y + Lu)	
	Nominal	Real	Nominal	Real
1.25	0.625	0.63	1.00	0.87
1.50	0.75	0.76	1.00	0.89
1.66	0.83	0.82	1.00	0.88
1.80	0.90	0.90	1.00	0.87
2.00	1.00	1.00	1.00	0.92

Data obtained from XRF analyses.

2.4. Characterization

The global composition of the samples was examined by X-ray fluorescence (X Siemens SRS-3000) in the gel calcined at 500 °C (xerogels); Table 1 shows the nominal and real compositions obtained; real Y/(Y + Lu) ratios show always a good agreement with the nominal compositions, while the Si/(Y + Lu) ratios indicate a Si content lower than that expected for the $Lu_{2-x}Y_xSi_2O_7$ stoichiometry. On the other hand, the chemical homogeneity of each sample was studied by TEM (TEM, Philips 200 CM); a number of single crystals were selected and EDX spectra (Philips DX4 equipment attached to the microscope) were recorded on each one, showing the spectra of the same sample very similar Y, Lu and Si contents. Several complementary techniques were selected which allowed a detailed ex situ characterization of the xerogels calcined at different temperatures. X-ray diffraction (XRD) studies were carried out using a Siemens D-501 diffractometer, with Ni-filtered Cu Kα radiation, steps of 0.05° and counting time of 5 s. Selected XRD patterns (recorded with 0.02° steps and 10 s counting time) were analyzed using the Le Bail method with the GSAS software (Larson and Von Dreele).[30] Refined parameters were: background coefficients, phase fractions, lattice constants, line widths and asymmetry parameters. Powder elemental silicon mixed with the sample was used as internal standard. ^{29}Si Magic Angle Spinning Nuclear Magnetic Resonance (MAS NMR) spectroscopy was carried out in a Bruker DRX400 AVANCE (9.39 T) spectrometer equipped with a multinuclear probe, using 4 mm zirconia rotors spinning at 11.5 kHz. A single pulse sequence was used, with an observation frequency for ^{29}Si of 79.49 MHz, a pulse width of 2.5 μs ($\pi/2$ pulse length = 7.5 μs) and a delay of 600 s.[27] Chemical shifts are reported in ppm from tetramethylsilane (TMS).

3. Results and discussion

3.1. Phase transitions in $Lu_{2-x}Y_xSi_2O_7$ ($1.25 \leq \times \leq 2$) as a function of temperature and composition

Fig. 1 shows representative portions of the XRD patterns of the $Lu_{2-x}Y_xSi_2O_7$ sample with $x = 2$ at different temperatures and calcination times. After annealing the xerogel at

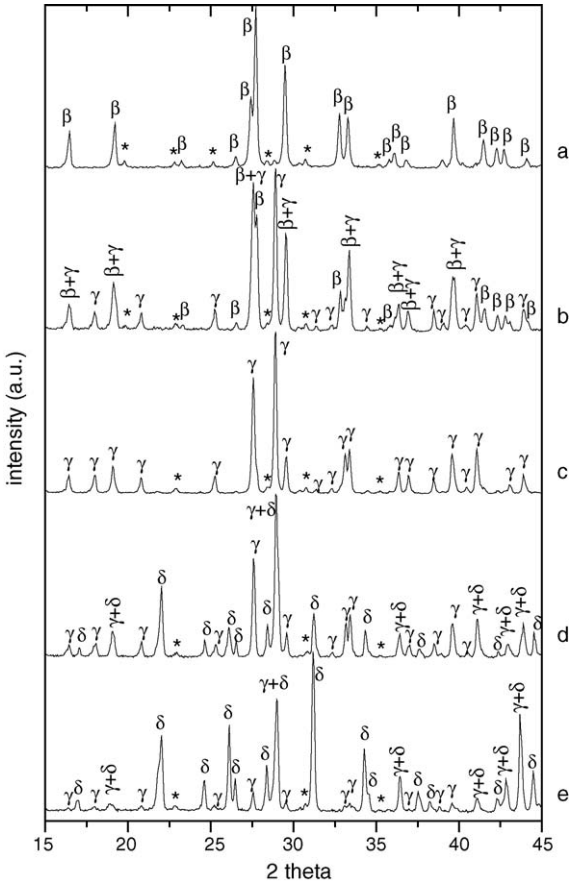

Fig. 1. Selected portions of the X-ray diffraction patterns of the $Lu_{2-x}Y_xSi_2O_7$ ($x=2$) xerogel calcined at (a) 1400 °C for 12 h, (b) 1400 °C for 36 h, (c) 1500 °C for 24 h, (d) 1650 °C for 12 h and (e) 1650 °C for 36 h. β = β-$Y_2Si_2O_7$, γ = γ-$Y_2Si_2O_7$, δ = δ-$Y_2Si_2O_7$, * = X2-Y_2SiO_5.

1400 °C for 12 h (Fig. 1a), the reflections match the JCPDS Card 38–440, corresponding to β-$Y_2Si_2O_7$. Some low-intensity reflections corresponding to X2-Y_2SiO_5 (marked with asterisks) are also observed, possibly as a result of the real composition of the sample (see Table 1). After 24 h more annealing at 1400 °C (Fig. 1b), the structure partially transforms to γ-$Y_2Si_2O_7$ (JCPDS Card 42–167); this observation indicates that γ-$Y_2Si_2O_7$ must be the thermodynamically stable phase at 1400 °C, although the transformation kinetics is still slow at this temperature. The β → γ transition temperature in pure $Y_2Si_2O_7$ can be located, therefore, at a temperature in between 1300 and 1400 °C, to be compared with the transition temperature of 1445 °C given by Ito and Johnson.[25] After annealing the xerogel at 1500 °C for 12 h (XRD not shown), γ-$Y_2Si_2O_7$ appears as the main phase, accompanied by traces of β-$Y_2Si_2O_7$. Annealing 24 h more at 1500 °C produces the complete transformation of β-$Y_2Si_2O_7$ into γ-$Y_2Si_2O_7$ (Fig. 1c) and this phase stays stable up to 1650 °C, temperature at which the partial transformation to δ phase occurs after 12 h annealing (Fig. 1d). Complete transformation of γ-$Y_2Si_2O_7$ into δ-$Y_2Si_2O_7$ is not observed even after further annealing at 1650 °C for 24 h (Fig. 1e). This fact indicates the sluggishness of the reconstructive transformations even at temperatures close to the melting point of the solid (1775 °C). Finally, it is interesting to note that no signs of δ-$Y_2Si_2O_7$ are observed at temperatures below 1650 °C, as opposed to the γ-$Y_2Si_2O_7$ → δ-$Y_2Si_2O_7$ transition temperature of 1535 °C reported in reference [25]. Based on our data, the γ → δ transition temperature is 1625(25) °C.

The behaviour of the $Lu_{2-x}Y_xSi_2O_7$ members with $1.25 \leq x < 2$ has been summarized in Table 2, which displays the phases observed in the XRD patterns of the samples calcined at each temperature for 12 and 36 h. The $Lu_{2-x}Y_xSi_2O_7$ member with $x = 1.25$ shows, exclusively, the β-polymorph after calcination at any temperature. The member with $x = 1.5$ crystallizes as β-polymorph at temperatures ≤1500 °C and the XRD pattern only shows some reflections corresponding to γ after annealing at 1600 °C for 12 h. Transformation to δ-polymorph is not observed at the highest temperature (1650 °C). The $x = 1.66$ member behaves in a similar way to the former composition, although in this case, the main phase observed after annealing at 1600 °C for 12 h is γ instead of β. The $x = 1.80$ member crystallizes as β-polymorph at temperatures ≤1400 °C, and it shows partial transformation to γ after calcination at 1500 °C for 12 h. At 1650 °C, γ still appears as the stable structure, even after the long calcination experiment. Based on data in Table 2, we have elaborated Table 3 with the β → γ and γ → δ transition temperatures for each composition.

3.2. Solid solubility of $Lu_2Si_2O_7$ in γ-$Y_2Si_2O_7$.

Fig. 2 shows the XRD patterns of the samples with $x \geq 1.5$ calcined at 1600 °C for 36 h; the patterns are very similar to each other and match the JCPDS Card of γ-$Y_2Si_2O_7$

Table 2
$Lu_{2-x}Y_xSi_2O_7$ polymorphs obtained after calcination of the xerogels at different temperatures and times

T (°C)	x									
	1.25		1.5		1.66		1.80		2.00	
	12 h	36 h	12 h	36 h	12 h	36 h	12 h	36 h	12 h	36 h
1400	β	β	β	β	β	β	β	β	β	γ + β
1500	β	β	β	β	β	β	γ + β	γ	γ + β	γ
1600	β	β	β + γ	γ[a]	γ + β	γ[a]	γ	γ[a]	γ	γ[a]
1650	β	β	γ	γ	γ	γ	γ	γ	γ + δ	δ + γ

In the cases of two polymorphs, the one written in the first place is the most abundant.
[a] Indicates samples submitted to reversibility studies.

Table 3
β → γ and γ → δ transition temperatures in the system $Lu_{2-x}Y_xSi_2O_7$ ($1.25 \leq x \leq 2.00$)

Type of transition	x				
	1.25	1.50	1.66	1.80	2.00
β → γ	n.o.	1550(50) °C	1550(50) °C	1450(50) °C	1350(50) °C
γ → δ	n.o.	n.o.	n.o.	n.o.	1625(25) °C

n.o. = not observed within the temperature range of our experiments.

(42–167) with slight variations in peak positions and intensities from one composition to the other. These variations result from changes in unit cell dimensions and unit cell contents. No reflections corresponding to β-$Lu_2Si_2O_7$ (JCPDS Card No. 35–326) are observed in any of the XRD patterns. Therefore, $Lu_2Si_2O_7$ does not segregates from $Y_2Si_2O_7$ as β-$Lu_2Si_2O_7$ but a unique phase (γ) is formed, at least from a long-range order point of view, in the compositional range $1.5 \leq x \leq 2$ at 1600 °C. This fact indicates that even though pure $Lu_2Si_2O_7$ forms a unique polymorph in the whole temperature range (β),[17] there is some degree of solid solubility of $Lu_2Si_2O_7$ in γ-$Y_2Si_2O_7$.

To confirm the solid solubility of $Lu_2Si_2O_7$ in γ-$Y_2Si_2O_7$ in the compositional range $1.5 \leq x \leq 2$ at 1600 °C, we have calculated the unit cell parameters of samples in Fig. 2 using the Le Bail method, as described in the experimental section. The starting parameters were those reported for pure γ-$Y_2Si_2O_7$.[20] All the reflections could be fitted on the basis of a monoclinic unit cell with space group $P2_1/c$, corresponding to the crystal structure of the γ-rare earth disilicates.[20] The lattice parameters as a function of Y content are shown in Fig. 3. The same size of the *y*-axis has been used in the three plots to appreciate relative changes in *a*, *b* and *c* parameters. Both *b* and *c* lattice parameters increase linearly with increasing Y content, while the *a* parameter does not change appreciably with composition. The *β* angle of the unit cell varies very little from one composition to the other, the maximum variation being of 0.03°. Finally, a linear dependence of the volume with the Y content is observed. The linear behaviour of the unit cell parameters with composition is a clear indication of the solid solubility of $Lu_2Si_2O_7$ in γ-$Y_2Si_2O_7$ in the compositional range $1.50 \leq x \leq 2.00$ at high temperatures.

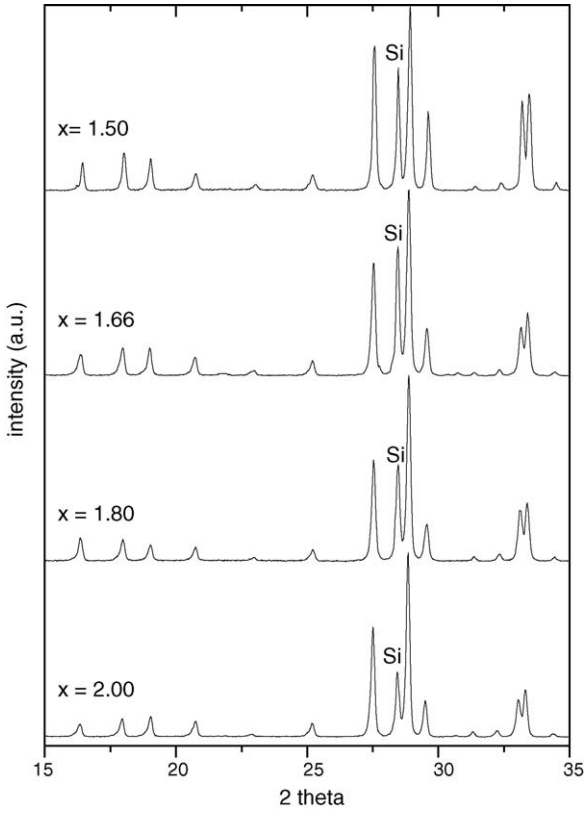

Fig. 2. Selected portions of the X-ray diffraction patterns of the $Lu_{2-x}Y_xSi_2O_7$ samples calcined at 1600 °C for 36 h, showing the γ modification. Si indicates Silicon used as internal standard.

3.3. Temperature–composition diagram of the $Lu_2Si_2O_7$–$Y_2Si_2O_7$ system

Previous structural studies on $Lu_2Si_2O_7$ and $Y_2Si_2O_7$ have shown that:

(i) Pure $Lu_2Si_2O_7$ exhibits exclusively the β-polymorph along the temperature range 900 °C < *T* < 1600 °C.[17]
(ii) $Lu_{2-x}Y_xSi_2O_7$ with $x = 1.00$ displays also exclusively the β-polymorph as the stable phase in the temperature range 1300 °C ≤ *T* ≤ 1650 °C.[28]
(iii) A solid solution is formed between β-$Lu_2Si_2O_7$ and β-$Y_2Si_2O_7$ at 1300 °C.[27]

Based on these data and on the results of the present study, and being cautious about the questionability of the equilibrium curves in the case of reconstructive transitions, we have summarized in Fig. 4 the behaviour of the $Lu_2Si_2O_7$–$Y_2Si_2O_7$ system as a function of temperature and composition. In order to obtain two more data points, which allow drawing the γ → δ boundary, two extra compositions close to the end-member ($x = 1.86$ and 1.92) were synthesized and annealed at high temperatures (maximum of 1700 °C) until observation of XRD peaks corresponding to the δ-polymorph. The sample with $x = 1.92$ showed peaks of δ-polymorph after annealing at 1675 °C while the sample with $x = 1.86$ needed a temperature of 1700 °C to show crystallization of δ-polymorph.

The boundaries of adjacent stability field of phases are based on data obtained from the synthesis of the compounds. The transition temperatures of the polymorphs, obtained from

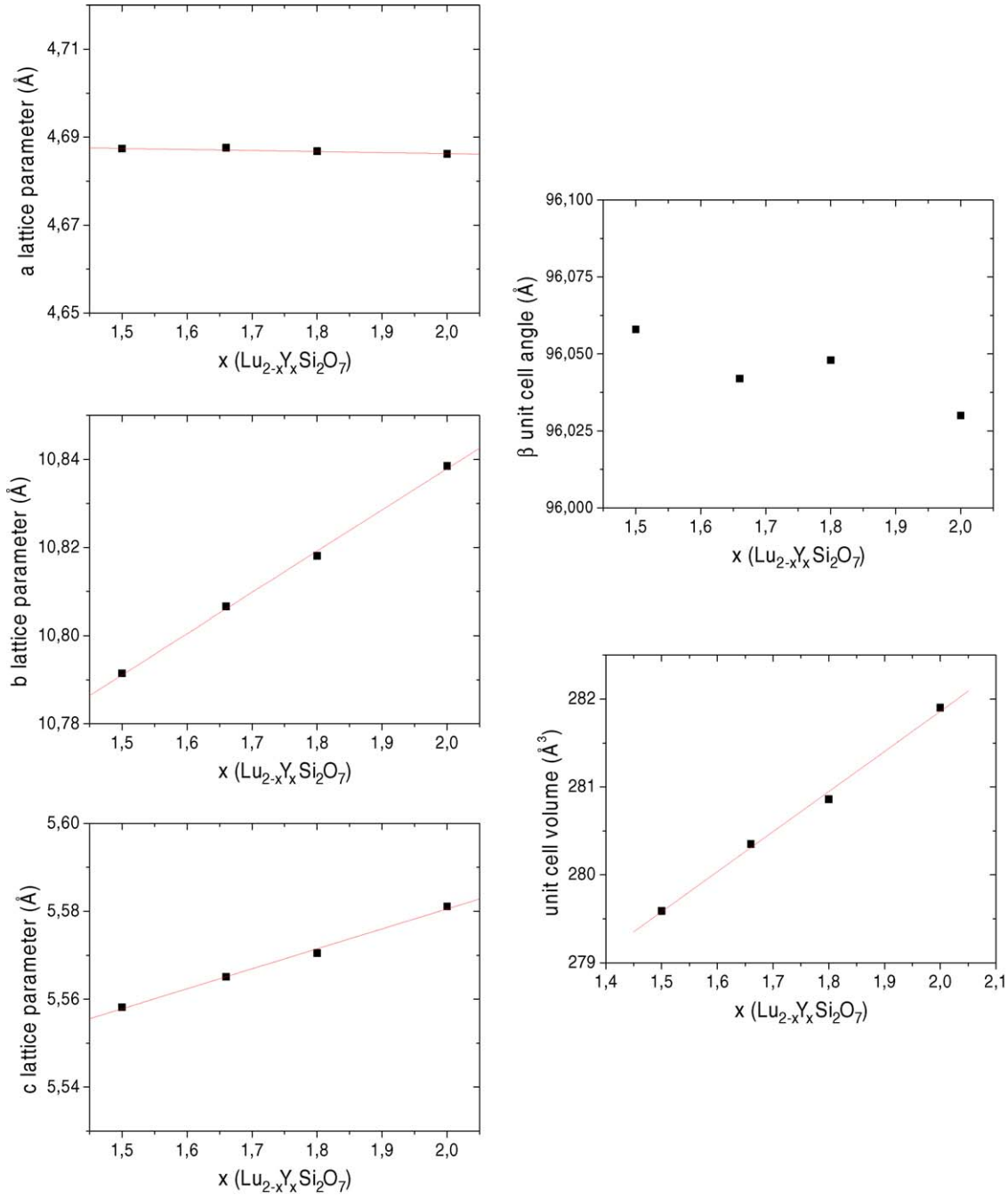

Fig. 3. Unit cell parameters (*a*, *b*, *c*, β and volume) plotted as a function of Y content obtained for $Lu_{2-x}Y_xSi_2O_7$ samples crystallizing as γ-polymorph. The error bars are approximately the size of the symbols.

annealing experiments, in which each phase is intended to be converted into the other, might differ slightly from these data. The diagram is dominated by the β-polymorph, displaying γ- and δ-polymorphs more reduced stability fields, especially the δ field. In conclusion, the structure of the β-polymorph, the unique shown by the $Lu_2Si_2O_7$ end-member, is the most stable in the $Lu_2Si_2O_7$–$Y_2Si_2O_7$ system; Lu(III) is able to share the RE crystallographic sites with Y(III) not only in the β-$RE_2Si_2O_7$ polymorph, but also in both γ- and δ-$RE_2Si_2O_7$, the latter only at low Lu concentrations and high temperatures.

3.4. Reversibility of the $\gamma \rightarrow \beta$ transition

Ito and Johnson[25] observed only a reverse reaction from δ-$Y_2Si_2O_7$ to γ-$Y_2Si_2O_7$ within a reasonable time of heating at slightly below the transition temperature. This result agrees well with the analysis of Felsche[17] for lanthanide pyrosili-

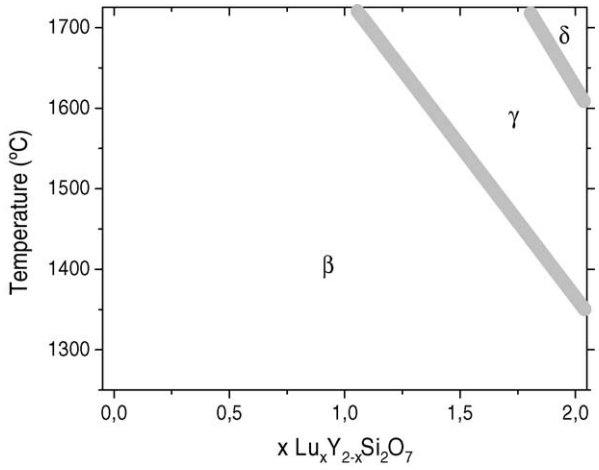

Fig. 4. Temperature–composition diagram of the $Lu_2Si_2O_7$–$Y_2Si_2O_7$ system based on data from this study and from our previous studies published in [27] and [28].

cates, where, in general, a large time constant is observed for the high- to low-form transitions. Some of the transitions were never observed within a reasonable period of time, i.e., within 100 h of observation. This is the case of the $\gamma \rightarrow \beta$ of $Ho_2Si_2O_7$, which shows the same four high temperature polymorphs as $Y_2Si_2O_7$.

In this study, we have analysed the influence of the Lu content on the reversibility of the $\gamma \rightarrow \beta$ transition in $Y_2Si_2O_7$, if any. Samples crystallizing as γ-$Lu_{2-x}Y_xSi_2O_7$ with $x = 1.50$, 1.66, 1.80 and 2.00 (samples used have been marked with asterisks in Table 2) have been annealed for 240 h at 1300 °C, temperature at which the β-polymorph is the stable phase for all the compositions.[27] Fig. 5 (left) shows the XRD patterns of the $Lu_{0.5}Y_{1.5}Si_2O_7$ sample before and after the reversibility experiment, as well as the XRD typical of β-$Lu_{0.5}Y_{1.5}Si_2O_7$ (taken from reference [27]). It can be seen that the patterns before and after the reversibility experiment are very similar and no diffraction corresponding to β-$Lu_{0.5}Y_{1.5}Si_2O_7$ is observed. The same behaviour is observed in the X-ray diffraction patterns of the other compositions of the system. To check whether any change has occurred in the local order of the structures, we have registered the ^{29}Si MAS NMR spectra of the samples before and after the reversibility experiment. Fig. 5 (right) shows both spectra for the case of $Lu_{0.5}Y_{1.5}Si_2O_7$ as well as the spectrum corresponding to β-$Lu_{0.5}Y_{1.5}Si_2O_7$ (plot *c*, taken from reference [27]); the starting sample (γ-$Lu_{0.5}Y_{1.5}Si_2O_7$) – plot *a* – shows a peak centred at a chemical shift of −92.2 ppm. Pure γ-$Y_2Si_2O_7$ exhibits a ^{29}Si chemical shift of −92.7 ppm[19] and the difference between this value and that presented by γ-$Lu_{0.5}Y_{1.5}Si_2O_7$ is due to the presence of both Y and Lu in crystal structure, as observed for β-$Lu_{2-x}Y_xSi_2O_7$ structures.[27] The ^{29}Si MAS NMR spectrum of the sample calcined at 1300 °C for 240 h – plot *b* – shows a peak centred at the same chemical shift (−92.2 ppm), indicating the absence of any appreciable change in the local order of the structure. The ^{29}Si MAS NMR spectrum of β-$Lu_{0.5}Y_{1.5}Si_2O_7$ has been included as plot *c* to show the chemical shift expected in case of a reversible transformation of γ-$Lu_{0.5}Y_{1.5}Si_2O_7$ to β-$Lu_{0.5}Y_{1.5}Si_2O_7$. The same behaviour is observed in the ^{29}Si MAS NMR spectra of the other compositions studied. In summary, the combination of XRD and ^{29}Si MAS NMR data allows concluding that the $\gamma \rightarrow \beta$ transition does not seem to take place either in pure γ-$Y_2Si_2O_7$ or in Lu-doped γ-$Y_2Si_2O_7$, at least within 10 days heating.

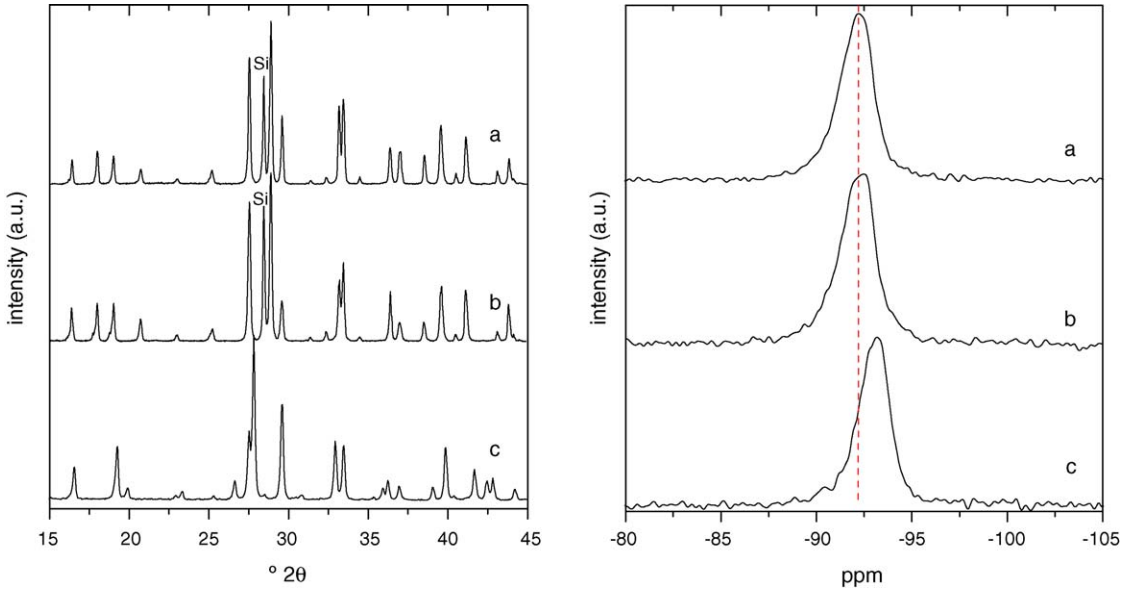

Fig. 5. X-ray diffraction patterns (left) and ^{29}Si MAS NMR spectra (right) of (a) γ-$Lu_{2-x}Y_xSi_2O_7$ with $x = 1.5$, (b) sample *a* calcined at 1300 °C for 240 h, (c) β-$Lu_{2-x}Y_xSi_2O_7$ with $x = 1.5$ (taken from reference [27]).

Acknowledgements

We gratefully acknowledge T.C. Rojas for help with TEM and the financial support from DGICYT Projects no. CTQ2004-05113 and MAT2002-03504 and Ramón y Cajal no. 2002/969.

References

1. Sanders, W. A. and Mieskowski, D. M., Strength and microstructure of sintered Si_3N_4 with rare-earth-oxide additions. *Am. Ceram. Soc. Bull.*, 1985, **64**, 304.
2. Cinibulk, M. K., Thomas, G. and Johnson, S. M., Grain-boundary-phase crystallization and strength of silicon-nitride sintered with a YSiAlON glass. *J. Am. Ceram. Soc.*, 1990, **73**, 1606.
3. Choi, H. J., Lee, J. G. and Kim, Y. W., Oxidation behavior of hot-pressed Si_3N_4 with Re_2O_3 (Re = Y, Yb, Er, La). *J. Eur. Ceram. Soc.*, 1999, **19**, 2757.
4. Cinibulk, M. K., Thomas, G. and Johnson, S. M., Strength and creep-behavior of rare-earth disilicate silicon-nitride ceramics. *J. Am. Ceram. Soc.*, 1992, **75**, 2050.
5. Nishimura, T., Mitomo, M. and Suematsu, H., High temperature strength of silicon nitride ceramics with ytterbium silicon oxynitride. *J. Mater. Res.*, 1997, **12**, 203.
6. Moulson, A. J., Reaction-bonded silicon-nitride – its formation and properties. *J. Mater. Sci.*, 1979, **14**, 1017.
7. Drew, P. and Lewis, M. H., Microstructures of silicon-nitride ceramics during hot-pressing transformations. *J. Mater. Sci.*, 1974, **9**, 261.
8. Lloyd, D. E., *Special Ceramics*, *Vol. 4*, ed. P. Popper. British Ceramic Research Association, Stoke-on-Trent, England, 1968, pp. 165–172.
9. Wild, S., Grieveson, P., Jack, K. H. and Latimer, M. J., *Special Ceramics*, *Vol. 5*, ed. P. Popper. British Ceramic Research Association, Stoke-on-Trent, England, 1972, pp. 377–384.
10. Tsuge, A., Nishida, K. and Komatse, M., Effect of crystallizing grain-boundary glass phase on high-temperature strength of hot-pressed Si_3N_4 containing Y_2O_3. *J. Am. Ceram. Soc.*, 1975, **58**, 323.
11. Drummond, C. H., Lee, W. E., Sanders, W. A. and Kiser, J. D., Crystallization and characterization of Y_2O_3–SiO_2 glasses. *Ceram. Eng. Sci. Proc.*, 1988, **9**, 1343.
12. Dinger, T. R., Rai, R. S. and Thomas, G., Crystallization behavior of a glass in the Y_2O_3–SiO_2–AlN system. *J. Am. Ceram. Soc.*, 1988, **71**, 236.
13. Arita, I. H., Wilkinson, D. S. and Purdy, G. R., Crystallization of yttria alumina silica glasses. *J. Am. Ceram. Soc.*, 1992, **75**, 3315.
14. Vomacka, P. and Babushkin, O., Yttria–alumina–silica glasses with addition of zirconia. *J. Eur. Ceram. Soc.*, 1995, **15**, 921.
15. Hong, Z. L., Yoshida, H., Ikuhara, Y., Sakuma, T., Nishimura, T. and Mitomo, M., The effect of additives on sintering behavior and strength retention in silicon nitride with RE-disilicate. *J. Eur. Ceram. Soc.*, 2002, **22**, 527.
16. Choi, H. J., Lee, J. G. and Kim, Y. W., High temperature strength and oxidation behaviour of hot-pressed silicon nitride disilicate ceramics. *J. Mater. Sci.*, 1997, **32**, 1937.
17. Feslche, J., Polymorphism and crystal data of rare-earth disilicates of type $Re_2Si_2O_7$. *J. Less Common Met.*, 1970, **21**, 1.
18. Feslche, J., The crystal chemistry of rare-earth silicates. *Struct. Bonding*, 1973, **13**, 100.
19. Parmentier, J., Bodart, P. R., Audoin, L., Massouras, G., Thompson, D. P., Harris, R. K. *et al.*, Phase transformations in gel-derived and mixed-powder-derived yttrium disilicate, $Y_2Si_2O_7$, by X-ray diffraction and Si-29 MAS NMR. *J. Solid State Chem.*, 2000, **149**, 16.
20. Christensen, N., Hazell, R. G. and Hewat, A. W., Synthesis, crystal growth and structure investigations of rare-earth disilicates and rare-earth oxyapatites. *Acta Chem. Scand.*, 1997, **51**, 37.
21. Tzvetkov, G. and Minkova, N., Influence of mechanical activation effect on the $Y_2Si_2O_7$ formation. *J. Mater. Sci. Lett.*, 2001, **20**, 1273.
22. Leonyuk, N. I., Belokoneva, E. L., Bocelli, G., Righi, L., Shvanskii, E. V., Henrykhson, R. V. *et al.*, High-temperature crystallization and X-ray characterization of Y_2SiO_5, $Y_2Si_2O_7$ and $LaBSiO_5$. *J. Cryst. Growth*, 1999, **205**, 361.
23. Dias, H. W., Glasser, F. P., Gunwardane, R. P. and Howie, R. A., The crystal-structure of delta-yttrium pyrosilicate, delta-$Y_2Si_2O_7$. *Z. Kristallogr.*, 1990, **191**, 117.
24. Dupree, R., Lewis, M. H. and Smith, M. E., High-resolution Si-29 nuclear magnetic-resonance in the Y–Si–O–N system. *J. Am. Chem. Soc.*, 1988, **110**, 1083.
25. Ito, J. and Johnson, H., Synthesis and study of yttrialite. *Am. Miner.*, 1968, **53**, 1940.
26. Becerro, A. I., Naranjo, M., Alba, M. D. and Trillo, J. M., Structure-directing effect of phyllosilicates on the synthesis of *y*-$Y_2Si_2O_7$. Phase transitions in $Y_2Si_2O_7$. *J. Mater. Chem.*, 2003, **13**, 1835.
27. Becerro, A. I. and Escudero, A., XRD and ^{29}Si MAS-NMR spectroscopy across the β-$Lu_2Si_2O_7$–β-$Y_2Si_2O_7$ solid solution. *J. Solid State Chem.*, 2005, **178**, 1.
28. Becerro, A. I. and Escudero, A., Phase transitions in Lu-doped $Y_2Si_2O_7$ at high temperatures. *Chem. Mater.*, 2005, **17**, 112.
29. Díaz, M., García-Cano, I., Mello-Castanho, S., Moya, J. S. and Rodríguez, M. A., Synthesis of nanocrystalline yttrium disilicate powder by a sol–gel method. *J. Non-Crystallogr. Solids*, 2001, **289**, 151.
30. Larson, A. C. and Von Dreele, R. B., *GSAS: General Structural Analysis System*. The Regents of the University of California, Los Alamos National Laboratory, Los Alamos, NM, 1994.